Carbon Dioxide Uptake Rate and Extent during Accelerated Curing of Concrete

S. Ghoshal[1], R.A. Niven[1],
[1]*McGill University, Montréal, Canada*

Carbon dioxide accelerated concrete curing process provides superior performance concrete masonry units, while eliminating harmful CO_2 emissions. This research investigates physiochemical changes affecting the rate, depth and extent of CO_2 uptake during the accelerated curing process using a flow-through reactor where moist CO_2 and N_2 (model flue gas) were passed through simulated concrete masonry units under ambient conditions. The CO_2 uptake dynamics demonstrated rapid and complete uptake in the early stages of carbonation. Declining uptake was observed in the second stage as a result of ongoing product layer deposition within the matrix. The loss of exposed and unreacted cement particle surface area from calcite deposition, hydration time (aging) and CO_2 flux were the main factors controlling the rate and extent of carbonation. Comparable CO_2 capture efficiency (17 %), kinetics of CO_2 uptake and superior depth of carbonation were obtained within one hour using as-captured flue gas under mild conditions with the flow-through reactor in comparison to pressure chamber type accelerated concrete carbonation methods. Enhancing the surface area of the grout material yielded near complete capture efficiency (79%).

1. Introduction

The observed effects of global warming, including rising sea levels, glacial retreat, species extinction, habitat loss, the spread of diseases and extreme weather events have been attributed to rising atmospheric levels of greenhouse gases (GHGs) [1]. In particular, CO_2 has been identified as the major anthropogenic contributor to the greenhouse effect which leads to global warming. The unprecedented levels of atmospheric CO_2 (365 ppm) are a result of rapidly increasing fossil fuel consumption since the beginning of the industrial era [2]. The Kyoto Protocol is the international response to combating the damaging effects of climate change. The protocol offers signatory nations a set of emission reduction targets and carbon offset and trading mechanisms. Under the protocol, Canada is bound to reduce its CO_2 emissions within the 2008-2012 compliance

[1] Corresponding author: Department of Civil Engineering, McGill University, 817 Sherbrooke Street West, Montreal, QC H3A 2K6, Canada. e-mail: subhasis.ghoshal@mcgill.ca

period by an average of 6% below the 1990 level. Achieving these ambitious goals will require a multifaceted approach involving the use of low carbon fuel sources, energy conservation, land use management and technical innovations such as carbon dioxide capture and storage (CCS).

CCS is a broad term that incorporates all engineered processes which involve capturing, transporting and storing CO_2 from large industrial emission point sources [3, 4]. The processes are intended to eliminate CO_2 emissions from polluting processes such as power or cement production plants. It is predicted to account for between 15 to 55% of the global CO_2 mitigation effort preceding 2100 [4]. CO_2 accelerated concrete curing is an alternative pre-cast concrete curing process that employs a form of CCS called mineral carbonation to safely and permanently store CO_2 as thermodynamically stable mineral carbonates within the concrete porous matrix. In addition to being a powerful CO_2 mitigation technology it also offers superior concrete physical properties and improved process conditions in comparison to conventional steam curing.

The chemical changes occurring during natural concrete weathering is comparable to that of CO_2 accelerated concrete curing. In both processes concrete is capable of sequestering approximately 50% of the cement mass as carbon dioxide [5]. Weathering reaction kinetics are, however, very slow compared to the CO_2 uptake reaction kinetics for accelerated concrete curing, where CO_2 sequestration reactions may be completed within hours. Nearly half of the global cement supply (1.1 Gt/yr) is used to produce products that are eligible for CO_2 accelerated concrete curing, which include: precast non-reinforced load-bearing or non-load-bearing concrete products such as concrete blocks, siding panels, roofing tiles, bricks, cement board, fiberboard, wall panels and concrete pipes [6]. With a low carbon intensity of 0.13 t CO_2 / t concrete, concrete products are already emission-competitive with other building materials [7]. Based solely on cement consumption and without even considering the sizeable CO_2 emission savings from eliminating steam or heat treatment, the process has the global potential to permanently and safely sequester up to 550 Mt CO_2 /yr while producing superior concrete products in less time than traditionally cured products. It has been found that concrete samples cured with this process benefit from greater volume stability, lower permeability, much faster 28-day strength development and enhanced compressive strength [8-12].

Previous research in the area has exhibited shallow CO_2 penetration depth, slow reaction kinetics and modest CO_2 uptake despite using severe process conditions. The research objectives of this project were to:

1. Design a model, flow-through concrete curing reactor that operates under ambient conditions and provides improved curing performance.

2. Define the factors limiting the rate, depth and extent of carbonation for the CO_2 accelerated concrete curing process.

3. Characterize the microstructural properties and classify the main constituents of the carbonated product.

4. Identify process parameters that influence the efficiency of CO_2 accelerated concrete curing.

Chemical and microstructural changes were investigated to clarify the previously unexplained limitations and provide solutions to enhance CO_2 storage and sample penetration.

2. Materials and Methods

2.1. Material Characterization and Preparation

Simulated concrete masonry units (CMUs) with a mass of 800g and a water cement ratio and dry density of 0.26 and 1.94 g/cm^3, respectively, were prepared with a cement grout mixture containing silica sand (Bromix), type 10 Portland cement (St. Lawrence Cement, Canada) and tap water. No coarse aggregate was used to improve sample homogeneity. A steel mold was constructed to cast cylindrical shaped grout samples with precise sample dimensions of 12.7 cm × 3.1 cm (d × h) and even distribution of the 8 MPa applied load. Within 2 hours after casting, the samples were mounted in a PVC shell using 5-minute epoxy. Prior to carbonation the mounted samples were stored in a sealed 100% humidity chamber at room temperature for predetermined aging periods.

Cement powder is a complex mixture of minerals and is the chemically reactive component in the grout mixture. The cement was characterized for its elemental composition using X-Ray Fluorescence (XRF) spectroscopy with a Phillips PW2440 4k W automated spectrometer, a AFT 6000/C automated fusion preparation system and a HERZOG HTP 40 pelletizing press. The particle size distribution of cement and silica sand were measured using a Lasentec M100 laser particle size analyzer and followed the ASTM LAS-W laser diffraction technique [13].

2.2. Reactor Design and Sample Carbonation

Two flow-through reactors were designed for carbonating the compacted and non-compacted grout samples. Previous research employed batch pressure chamber apparatus which required either/or high pressures and

temperatures, vacuum conditions, pure CO_2 and long experimental runs [14, 15]. The flow-through design provided equitable CO_2 uptake results and better penetration and kinetics, despite using ambient experimental conditions and simulated flue gases with low CO_2 partial pressures.

Carbonation experiments were conducted with certified high purity (± 0.1%) CO_2 gases in a nitrogen balance (Praxair Inc) in one of two reactors depending on the grout physical properties. Carbonation was tested under a range of ambient conditions (20-40% CO_2, 1-3.4 atm, 20ºC, 30-7000 min, 0.1-2 sLpm, 20-100% RH). In both reactor designs the system was operated at constant temperature, pressure, flow, CO_2 partial pressure and relative humidity. The first category, consisting of compacted grout samples, was carbonated in the 1-D flow-through reactor (Fig. 1A). Non-compacted samples were carbonated in a custom-made 250 mL pyrex glass three-port continuously-stirred, gas-sparged reactor (Fig. 1B). Depending on the experiment, the appropriate reactor was selected and connected to the overall apparatus. The apparatus included the gas control systems (pressure gauges, flow rate regulator, water trap and particulate filter), analytical instrumentation (temperature/relative humidity probe, CO_2 sensor) and certified gas supply (Fig. 1C). The reactors were submerged in a water bath during operation to maintain a constant temperature and check for leaks.

2.3. Analysis Techniques

The rate and extent of CO_2 uptake were tracked using two infrared (IR) gas absorption instruments. The first IR instrument, an Eltra CS-800 combustion infrared gas analyzer, offered direct and precise measurement of the total CO_2 uptake and moisture content of solid carbonated samples. CO_2 uptake dynamics were also monitored online using a Quantek model 906 NDIR CO_2 gas sensor. Data from the inline CO_2 sensor and a combined relative humidity and temperature probe were collected every 5 seconds for the duration of the experiment with a multi-channel datalogger.

Following the experiment, scanning electron microscopic analysis (SEM) was conducted with a Hitachi S 4700 field emission gun SEM (FE-SEM) equipped with a Robinson backscatter detector to identify the major morphology and spatial distribution of the reaction products. Grout samples were electrically grounded prior to the SEM analysis by applying a 400Å Au/Pd coating. X-Ray diffraction (XRD) analysis of the carbonated material was performed to identify the morphology of the main constituents with a Phillips PW 1710 powder XRD instrument and interpreted with the 2005 ICDD diffraction pattern library.

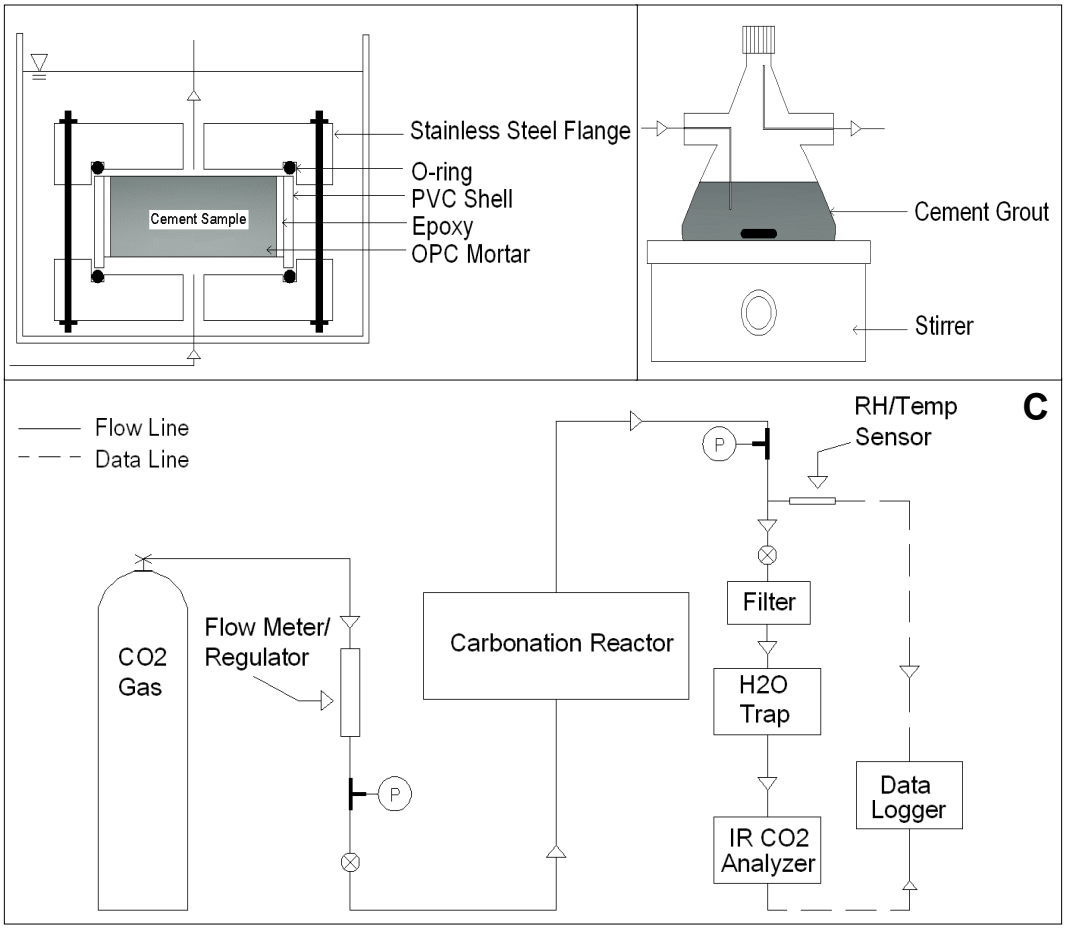

Figure 1. Carbonation apparatus (A) compacted grout reactor, (B) loose grout reactor, (C) overall carbonation apparatus setup.

2.4. Carbonation Efficiency Calculations

The Steinour formula (Eq. 1) estimates the theoretical limit of CO_2 sequestration in terms of the elemental composition of the raw materials [5]. The CO_2 uptake potential ($X_{CO_2\ Tot}$) in units of wt %, is a function of the relative mass of the specific metal oxides ($X_{CaO,\ MgO,\ SO_3,\ Na_2O,\ K_2O}$). Based on the relative mass of oxides within cement, the CO_2 uptake capacity ($X_{CO_2\ Tot}$) of cement was found to be 49.62 wt %.

$$X_{CO_2Tot} = 0.785(X_{CaO} - 0.700X_{SO_3}) + 1.091X_{MgO} + 1.420X_{Na_2O} + 0.935X_{K_2O} \quad (1)$$

The carbonation efficiency (ξ) (Eq. 2) was calculated to quantify the degree of carbonation normalized to the mass of cement contained within the product using the combustion infrared gas analysis data. It is defined

as the mass of sequestered CO_2 (M_{CO_2}) divided by the mass of the Steinour-derived theoretical uptake limit ($M_{CO_2\,Tot}$). Equation 2 is a function of the fraction sequestered CO_2 within the carbonated dry sample (X_{CO_2}), the 7.1 wt% fraction of the non-carbonated dry sample containing CO_2 ($X_{CO_2}^{o}$), the mass of the dry carbonated sample (M_P), the mass of cement (M_C) and the theoretical maximum CO_2 uptake capacity ($X_{CO_2\,Tot}$). An adjusted carbonation efficiency equation (Eq. 4) was devised, by applying equation 3, where M_F is the mass of fine aggregate (sand) and M_{CO_2} is the mass of sequestered CO_2. Equation 4 eliminates the errors affecting M_P associated with estimating the mass of net water gain and the grout material loss from handling. On average a carbonation efficiency of 16.7 ± 2.1% was measured for compacted grout samples using standard carbonating conditions.

$$x = \frac{M_{CO_2}}{M_{CO_2Tot}} = \frac{(X_{CO_2} - X_{CO_2}^{o}) * M_P}{X_{CO_2Tot} * M_C} \tag{2}$$

$$M_P = M_C + M_F + M_{CO_2} \tag{3}$$

$$x = \frac{(\frac{M_F}{M_C} + 1)}{X_{CO_2Tot}} * \frac{X_{CO_2} - X_{CO_2}^{o}}{1 - (X_{CO_2} - X_{CO_2}^{o})} \tag{4}$$

A second carbonation efficiency (ξ) calculation method (Eq. 6) was designed to offer real time CO_2 uptake tracking from the inline NDIR CO_2 data. The numerator of equation 2 was calculated by directly measuring the mass of sequestered CO_2 during the experiments by applying equation 5 with known flow (Q), measurement intervals (Δt = 5s), gas density (ρ_{CO_2}) and inlet ($C_{CO_2}^{o}$) and effluent (C_{CO_2}') CO_2 concentrations. The sum of all time intervals for the length of the experiment yielded the total CO_2 mass gain (M_{CO_2}). Substitute (M_{CO_2}) into equation 2 to gain the second carbonation efficiency measurement method (Eq. 6). The CO_2 uptake efficiency (ξ) calculated using the inline NDIR CO_2 measurements compared well with the efficiency computed with the combustion infrared analysis results.

$$M_{CO_2} = (C_{CO_2}^{o} - C_{CO_2}') * Q * \Delta t * r_{CO_2} \tag{5}$$

$$x = \frac{M_{CO_2}}{X_{CO_2Tot} * M_C} \tag{6}$$

3. Results and Discussion

3.1. CO_2 Uptake Dynamics

Two distinct stages in the CO_2 uptake patterns were observed during the carbonation of compacted and non compacted cement grout as displayed in a typical carbonation plot under standard conditions in Figure 2.The area between the inlet and effluent CO_2 concentration curves (Fig. 2A and 2B) illustrates the quantity of sequestered CO_2 as outlined in equation 5. During the course of this brief 30 minute period, all of the CO_2 was sequestered from the gas stream, demonstrating the fast kinetics and sequestration potential of cement products. The cumulative CO_2 mass gain (Fig. 2C) exemplifies the high proportion of sequestration occurring within this short period.

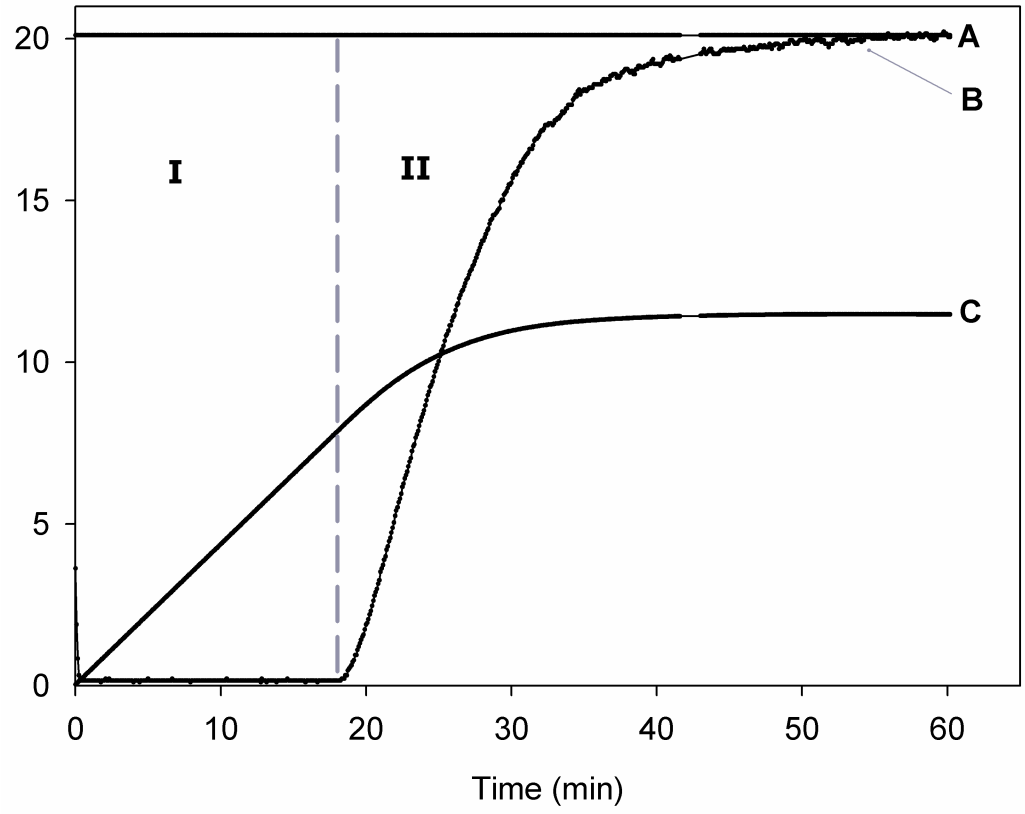

Figure 2. Carbonation plot of compacted cement grout. (A) inlet CO_2 concentration (%) , (B) outlet CO_2 concentration (%), (C) cumulative CO_2 mass gain (g). The error bar denotes the standard deviation (σ = 1).

Eventually stage I terminated, leading to the gradually declining and eventually insignificant uptake in stage II. The carbonation reaction ran to completion within one hour without reaching complete conversion. Long

term carbonation experiments (7 days) did not offer any significant CO_2 uptake or loss.

CO_2 accelerated concrete curing involves many concurrent microstructural and chemical changes. The reactions 7-10 represent the chemical changes that occur during the carbonation reaction. These include dissolution of CO_2 in water (Eq. 7a-c), calcium dissolution from cement and portlandite (Eq. 8 and 9), and the precipitation of calcium carbonate (Eq. 10). It has been proposed that (1) relative humidity [8], (2) CO_2 hydration kinetics [16], (3) portlandite deposition [17, 18], (4) $CaCO_3$ deposition [19-22] and (5) moisture content [11, 14, 15] are the main factors controlling the reaction dynamics in various lime and concrete carbonation experiments. The CO_2 accelerated concrete curing mechanism and the aforementioned proposed factors were studied to clarify the governing variables under a range of ambient conditions. It was found that $CaCO_3$ deposition, and in certain cases portlandite dissolution, were the governing factors controlling carbonation dynamics. The rate and extent of $CaCO_3$ deposition was a function of the exposed pore surface area, flow rate and CO_2 gas concentration. Doubling CO_2 flow or concentration reduced the length of stage I by 50% without lowering the uptake. In experimental work, the degree of portlandite deposition was modified by the length of grout aging period. The grout moisture content, chamber pressure, relative humidity and CO_2 hydration reaction rate were shown to have no significant effect on the reaction dynamics under the conditions studied.

$$CO_2(g) + H_2O \rightarrow H_2CO_3^* \quad (7a)$$

$$H_2CO_3^* \rightarrow HCO_3^- + H^+ \quad (7b)$$

$$HCO_3^- \rightarrow CO_3^{2-} + H^+ \quad (7c)$$

$$(CaO)_X \cdot SiO_2 \cdot nH_2O + 2yH^+ \rightarrow (CaO)_{x\cdot y} \cdot SiO_2 \cdot nH_2O + yCa^{2+} + yH_2O \quad (8)$$

$$Ca(OH)_2 \rightarrow Ca^{2+} + 2OH^- \quad (9)$$

$$Ca^{2+} + CO_3^{2-} \rightarrow CaCO_3 \downarrow \quad (10)$$

3.2. Effects Product Layer Deposition on Dynamics

Portlandite deposition and dissolution controlled the kinetics, extent and heterogeneity of carbonation reactions only when samples were sufficiently hydrated (aged) prior to carbonation. For this study, aging or hydration time refers to the elapsed time from when moisture is first added to the dry grout material until the sample is carbonated. During aging, hydration reactions (Eq. 11-12) form a portlandite product layer that caused a brief period of slower carbonation dynamics as observed in the

carbonation plots for aged and unaged samples in Figure 3. SEM images confirmed that the low permeability, yet ultimately soluble, portlandite product layer was extensively deposited throughout the grout matrix. This product layer limited CO_2 ingress into the porous network and imposed an ion diffusion controlled reaction rate which temporarily delayed carbonation until the product layer was slowly dissolved by carbonic acid (Eq. 13) as shown by the increasing uptake rate in the latter half of stage I (Fig. 3B) [17].

$$(CaO)_3 \cdot SiO_2 \cdot nH_2O + 2H^+ \rightarrow (CaO)_2 \cdot SiO_2 \cdot nH_2O + Ca^{2+} + H_2O \quad (11)$$

$$Ca^{2+} + 2OH^- \rightarrow Ca(OH)_2 \downarrow \quad (12)$$

$$Ca(OH)_2 \xrightarrow{H_2O} Ca^{2+} + 2OH^- \xrightarrow{CO_2} CaCO_3(s) + H_2O \quad (13)$$

The retarded CO_2 uptake was observed for aging periods longer than approximately 20 hours. Optimal carbonation results were obtained with minimal hydration time (2 hrs) (Fig. 3A), without compromising strength. The conventional 28-day strength rating can be attained in less than 20 minutes using the accelerated carbonation curing process [23].

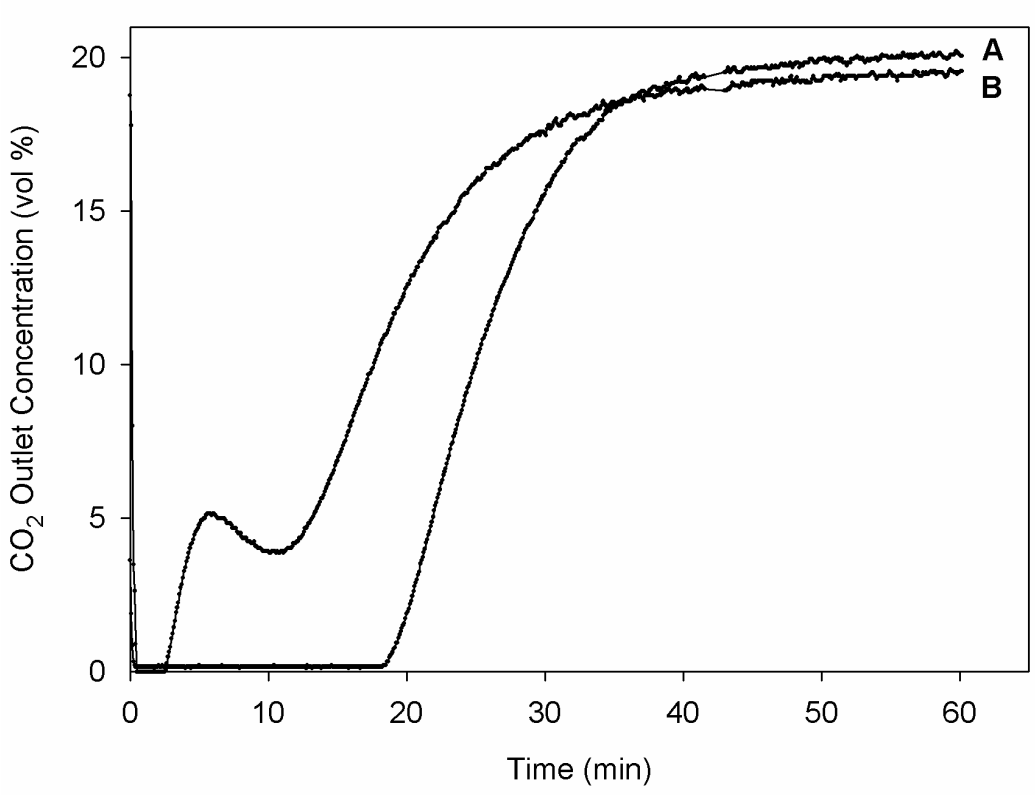

Figure 3. Carbonation effects from aging. (A) unaged grout and (B) aged grout. Error bars denote the standard deviation (σ = 1).

During stage I (Figure 2), CO_2 is rapidly replenished throughout the unsaturated pore network by advection to sustain the carbonation reactions (Eq. 7-10) [19]. The onset of stage II carbonation dynamics occur when the particle and pore surface area is coated with an impermeable $CaCO_3$ product layer that essentially halts ion diffusion. The process is analogous to portlandite deposition in that the precipitates will deposit within pores and on particle surfaces. The distinguishing effects between portlandite and calcite deposition are the ir relative solubilities. Portlandite is more soluble than calcite and will dissolve upon carbonation (Eq. 13) to form calcite. As such it will only impose a temporary ion transport limitation until it is sufficiently dissolved. Calcite ($CaCO_3$) is insoluble and thus will impose permanent ion diffusion and CO_2 uptake limitations.

Large kinetic gains were achieved by reducing the aging time and increasing the CO_2 flow rates and concentration of the as-captured flue gas used in the flow-through reactor. Without any attempt to promote CO_2 uptake in stage II, the kinetics and overall uptake can be enhanced by increasing the CO_2 supply rate and minimizing the aging time. Concentrating the flue gas to achieve higher CO_2 partial pressures is likely not as economically viable. Minimizing aging time poses no perceived disadvantages since aging time lengthens the industrial production cycle, thereby raising costs, and is not required for product strength development in accelerated concrete curing.

3.3. Extent of Carbonation

Loss of exposed surface area was identified as the main limiting factor governing the rate and extent concrete carbonation. Carbonation experiments were performed to investigate the effects of increased surface area on CO_2 uptake. Non-carbonated and compacted grout samples were crushed into loose material in order to expose the cement particle surface area and eliminate the particle-particle contact of closed, tortuous and narrow pores that would normally plug during carbonation and impede complete conversion. Typical standard samples (uncrushed) were prepared and carbonated under similar conditions as the crushed samples. The carbonation of the standard sample (compacted grout material) demonstrated a typical CO_2 uptake profile similar to Figure 2 with negligible uptake beyond the commencement stage II. The average carbonation efficiency (ξ) of the standards was $20.2 \pm 0.6\%$. Nearly full carbonation efficiency was reached within 40 min ($\xi = 78.7 \pm 9.7\%$) for the loose grout samples. Comparable carbonation efficiency ($\xi = 68.3 \pm 3.2\%$) was measured when a standard sample was crushed and recarbonated as a loose material. The results indicated that there was a remarkable three fold rise in carbonation efficiency from increasing the exposed cement particle surface area. Although the loose material achieved much

higher CO_2 uptake, it has little value as a construction material. Adjustments to the CO_2 accelerated concrete curing process that increase the surface area of cement particles for enhanced carbonation efficiency, such as modifications to the aggregates mix design, compaction pressure and the carbonation process, may provide increased carbonation.

4. References

[1] Masters, G.M., Introduction to Environmental Engineering and Science. 1997, Upper Saddle River, NJ: Prentice-Hall.

[2] IPCC, Climate Change 2001: The Scientific Basis. Contribution of Working Group I to the Third Assessment Report of the Intergovernmental Panel on Climate Change, J.T. Houghton, et al., Editors. 2001, Cambridge University Press: Cambridge, United Kingdom and New York, USA. p. 881.

[3] Anderson, S. and R. Newell, *Prospects for carbon capture and storage technologies.* Annual Review of Environment and Resources, 2004. **29**: p. 109-142.

[4] IPCC, *IPCC Special Report on Carbon Dioxide Capture and Storage*, B. Working Group III of the Intergovernmental Panel on Climate Change [Metz, O. Davidson, H. C. de Coninck, M. Loos, L. A. Meyer (eds.)], Editor. 2005, Cambridge University Press: New York. p. 442.

[5] Steinour, H.H., *Some effects of carbon dioxide on mortars and concrete-discussion.* J. Am. Concrete, 1959(30): p. 905.

[6] van Oss, H.G., *Mineral Commodity Summaries*, U.S.G. Survey, Editor. 2006.

[7] CPCA, *Concrete Contributions to Meeting Canada's Kyoto Commitment*, C.P.C. Association, Editor. 1998, Canadian Portland Cement Association: Ottawa.

[8] Papadakis, V.G., C.G. Vayenas, and M.N. Fardis, *Reaction engineering approach to the problem of concrete carbonation.* AIChE Journal, 1989. **35**(10): p. 1639-1650.

[9] Toennies, H.T., *Artificial carbonation of concrete masonry units.* American Concrete Institute -- Journal, 1960. **31**(8): p. 737-755.

[10] Lange, L.C., C.D. Hills, and A.B. Poole, *Preliminary investigation into the effects of carbonation on cement-solidified hazardous wastes.* Environmental Science and Technology, 1996. **30**(1): p. 25-30.

[11] Young, J.F., R.L. Berger, and J. Breese, *Accelerated Curing of Compacted Calcium Silicate Mortars on Exposure to CO_2.* Journal of the American Ceramic Society, 1974. **57**(9): p. 394-397.

[12] Freedman, S., Carbonation Treatment of Concrete Masonry Units. Modern Concrete, 1969. **33**(5): p. 33-6.

[13] Ferraris, C.F., V.A. Hackley, and A.I. Aviles, Measurement of particle size distribution in portland cement powder: Analysis of ASTM round robin studies. Cement, Concrete and Aggregates, 2004. **26**(2): p. 71-81.

[14] Reardon, E.J., B.R. James, and J. Abouchar, *High Pressure carbonation of cementitious grout.* Cement and Concrete Research, 1989. **19**(3): p. 385-399.

[15] Venhuis, M.A. and E.J. Reardon, *Vacuum method for carbonation of cementitious wasteforms.* Environmental Science and Technology, 2001. **35**(20): p. 4120-4125.

[16] Fernandez Bertos, M., et al., A review of accelerated carbonation technology in the treatment of cement-based materials and sequestration of CO_2. Journal of Hazardous Materials, 2004. **112**(3): p. 193-205.

[17] Van Balen, K., Carbonation reaction of lime, kinetics at ambient temperature. Cement and Concrete Research, 2005. **35**(4): p. 647-657.

[18] Shih, S.-M., et al., *Kinetics of the reaction of $Ca(OH)_2$ with CO_2 at low temperature.* Industr ial and Engineering Chemistry Research, 1999. **38**(4): p. 1316-1322.

[19] Abanades, J.C. and D. Alvarez, *Conversion limits in the reaction of CO_2 with lime.* Energy and Fuels, 2003. **17**(2): p. 308-315.

[20] Dewaele, P.J., E.J. Reardon, and R. Dayal, *Permeability and porosity changes associated with cement grout carbonation.* Cement and Concrete Research, 1991. **21**(4): p. 441-454.

[21] Bhatia, S.K. and D.D. Perlmutter, *Effect of the Product Layer on the kinetics of the CO_2-lime reaction.* AIChE Journal, 1983. **29**(1): p. 79-86.

[22] Huijgen, W.J.J., G.-J. Witkamp, and R.N.J. Comans, *Mineral CO_2 sequestration by steel slag carbonation.* Environmental Science and Technology, 2005. **39**(24): p. 9676-9682.

[23] Shideler, J.J., *Investigation of the moisture-volume stability of concrete masonry units.* Portland Cement Association, 1955. (D3).